

ON THE PREDICTION OF PILE DRIVING INDUCED UNDERWATER SOUND PRESSURE LEVELS OVER LONG RANGES

Tristan Lippert, Kristof Heitmann, Marcel Ruhnau, Stephan Lippert and Otto von Estorff

*Institute of Modelling and Computation, Hamburg University of Technology,
Hamburg, Germany
email: tristan.lippert@tuhh.de*

Underwater noise, radiated from pile driving at offshore wind farm construction sites, has become a major issue in the course of the recent reorganization of the energy supply in Germany. To predict the sound pressure levels (SPLs) of planned wind farms and to optimize the according noise insulation systems, the need for a numerical simulation tool has arisen. In this contribution, an envisaged global model, consisting of the detailed simulation of the pile/soil-interaction, the properties of insulation measures, and the prediction of SPL in large distances from the pile, is introduced. A basic finite element (FE) model is presented which models the pile itself and the surrounding water up to a distance of 50 m around the pile. This model is used to extract the acoustic source properties that are needed to couple the presented wavenumber integration (WI) code, which is utilized as a propagation method. The pile as an acoustic source is investigated in detail and feasible simplifications of the extracted output signals are suggested. Finally, the results of the WI model are compared to the FE results and an outlook on future research activities is given.

1. Introduction

Until a couple of years ago, pile driving induced underwater noise has been an issue mainly associated with the erection of near shore buildings or bridges and its effects on fish, see for example Stadler and Woodbury [1]. Today, this problem has reached a new level, both in quality and quantity, in the context of offshore wind farm constructions, with pile driving being the current state of the art foundation. Hereby, it combines the negative effects of the other two main sound sources in the ocean, namely seismic explorations and shipping noise. On the one hand, high sound pressure levels (SPLs) comparable to seismic explorations are encountered during the construction phase, with peak source SPLs of up to 228 dB¹, see for example Götz et al. [2]. On the other hand, due to the rapid development of offshore wind farms on the way to a more sustainable energy production, for Germany, see [3], parallel construction activities at several sites will lead to a continuous acoustic pollution of the according areas, as does shipping noise.

¹All dB values in this work are referenced to 1 μ Pa

To protect the marine environment several countries have already decreed different regulations, such as seasons of suspension in the Netherlands, to protect fish larvae, or whale watchers in the United Kingdom, see Koschinski and Lüdemann [4]. In Germany, the main concern is the protection of the already endangered harbour porpoise, wherefore limiting values of 190 dB for the peak sound pressure level (SPL_{peak}) and 160 dB for the sound exposure level (SEL), both measured at a distance of 750 m from the pile and 2 m above the sea floor, during the construction phase have been issued, cf. [5]. To observe these rules, sound insulation measures, such as bubble curtains or cofferdams, have to be applied during the operation of pile drivers.

In this context, the need to have a numerical simulation tool that correctly represents the acoustic radiation of pile driving, is mainly driven by two considerations. On the one hand, construction companies as well as approving authorities need a reliable prediction of the SPLs that can be expected from pile driving for planned future wind farms. On the other hand, an a priori optimization of sound insulation measures is desirable to minimize offshore testing costs.

This paper focuses on the ability of such a numerical model, to predict sound pressure levels in distances of several kilometers from the actual construction site. In section 2, the envisaged global model is described, as well as the finite element (FE) approach for the area close to the pile, and the physical principle governing the acoustic radiation in this context is exemplified. This near field model will be used subsequently to determine the input excitation for far field calculations and to verify the according results. In section 3, the wavenumber integration (WI) technique used for far field predictions is briefly introduced and the application to the given problem is elucidated. The coupling of the FE and WI model and the comparison of the results are discussed in section 4, before a conclusion and an outlook on planned research activities is given in section 5.

2. FE modelling of pile driving noise

Due to the large size of the area of interest and the high frequency regime that has to be considered, the numerical modelling of acoustic emissions from pile driving is computationally rather challenging. Looking at the German regulations mentioned above, the most important dimension of a model would be a radius larger than 750 m around the pile. Additionally, measurement guidelines that are in preparation also foresee the monitoring of nature reserves in distances of up to 5 km, see Müller and Zerbs [6], which would also have to be included in any useful numerical model. The upper frequency limit of interest for a modelling approach is still up for discussion. On the other hand, studies show that the auditory system of marine mammals, such as the harbour porpoise, can sense signals up to several kilohertz, see for example Kastelein et al. [7, 8]. On the other hand, measurement data indicate that the pulses, emitted during pile driving, do not have a significant energy content in the region roughly above 1 kHz, see for example Wilke et al. [9]. This characteristic is additionally amplified by the frequency dependent damping in sea water, that increases with frequency, see Brekhovskikh and Lysanov [10]. Taking this into account, the authors consider it a feasible approach to account for frequencies up to 2 kHz.

With these constraints, it becomes clear that a straight forward modelling approach, for example using the finite element method, is not practical, due to the number of degrees of freedom, resulting from the vast dimensions and the high frequency content. Therefore, a subdivided calculation of the whole system, as for example suggested by Stokes et al. [11], is desirable. The authors have chosen a tripartite modelling approach, consisting of a high fidelity FE model to simulate the complicated interaction of the hammer with the pile and the subsequent intrusion of the pile into the soil. This model is coupled to an acoustic FE model covering the first few meters around the pile, including possible sound mitigation measures. Finally, the results of this model are coupled to a propagation model, which allows for SPL prediction in large distances from the pile, using a number of simplifications. In this work, the main focus is on the propagation model and the determination of its input

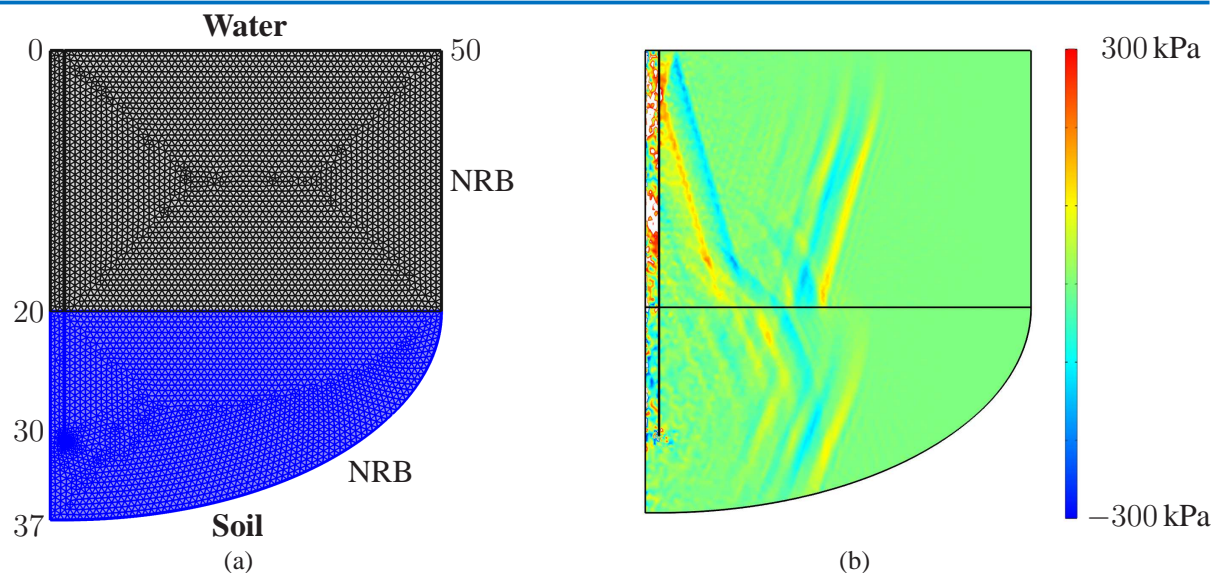


Figure 1. Finite element model used to determine the excitation for the propagation method and to verify the according results: (a) Basic model setup and dimensions in meters / (b) Pressure contours 12 ms after the hammer impact, showing the characteristically inclined wave fronts

signals, wherefore an FE model consisting of both the pile and its nearer surroundings is used.

The two-dimensional, axis-symmetric model can be found in figure 1(a). It consists of a pile with a diameter of $D = 2,1$ m and a total length of $L = 30$ m, whereof 20 m are surrounded by water and 10 m are embedded in the soil. Simplifying, the soil is assumed to be an equivalent fluid, representing a fine sand, see Hamilton [12]. Hence, the applied fluid properties are $\rho_W = 1000$ kg/m³ for the density and $c_W = 1453$ m/s for the speed of sound of the water, and $\rho_S = 1941$ kg/m³ and $c_S = 1749$ m/s for the soil. To fix the pile in the fluid soil, it is connected to spring-damper elements along its embedded length, which also govern the absorption of the mechanic energy put into the system by the hammer. To account for the half-infinite nature of the ocean as a waveguide, the outer limits of the model are enclosed by non-reflecting boundaries (NRBs). Due to the high difference in impedance between air and water, the air phase is not modelled here, and the ocean surface is assumed to be a perfect reflector with $R = -1$. The interaction between the hammer mass and the pile is considered, using an analytical model as suggested by Deeks and Randolph [13]. The analytically calculated forces are applied to the FE model via a force boundary condition at the top of the pile.

In figure 1(b), an exemplary pressure field contour, taken 12 ms after the hammer impact, is shown. The inclined wave fronts that are characteristic to pile driving, see for example by Reihnall and Dahl [14], can clearly be identified. The relatively short hammer impact triggers a longitudinal wave that is running down the pile, with a propagation speed of roughly $c_{imp} \approx 5100$ m/s. Due to the transversal contraction, i.e., Poissons' ratio, this also induces a transversal deformation wave, which in turn causes an excitation of the surrounding fluid und thereby acts as an acoustic source. The inclination of the wave fronts in water of about $\phi_{water} \approx 16^\circ$ can easily be calculated by the relation of the speed of sound in water c_{water} and the propagation velocity of the impulse c_{imp} . What is important here is the fact, that relative to the speed of sound in water, the impulse, i.e., the acoustic source, is traveling with supersonic speed. This leads not only to a standard Huygens wave front, formed by every aligned set of point sources, but to a high energetic Mach front. The second set of wave fronts, with opposite inclination, results from the impulse that has been reflected at the foot of the pile and travels up again. It can also be seen, that these reflections arrive with reversed phase, as the impedance in steel is significantly higher than in the equivalent fluid, representing the soil.

3. Wavenumber integration modelling of pile driving noise

As explained in section 2, a so-called propagation method is needed to predict SPLs in large distances from the acoustic source. Prominent representatives of this class of computational procedures are for example ray tracing algorithms, normal modes or parabolic equation modelling. Each of these methods involves a number of simplifications, and thereby constraints to its field of application. For a deeper insight into the mentioned approaches and a general overview, see for example Jensen et al. [15].

For the envisaged global model, a WI approach is used, in the form suggested by Schmidt and Tango [16] and Schmidt [17]. This technique is suitable for the frequency range of interest and gives results for a two-dimensional, multi-layered environment. Its most significant drawback is the difficulty to handle strong range-dependence, however this is considered a minor confinement, at least for the North Sea. Therefore, it computes the full field, including the evanescent spectrum, which might be of importance in connection with the prescribed measurement position close to the water/soil interface, mentioned in section 1. The formal derivation of the method is based on the Helmholtz equation for a two-dimensional, axis-symmetric, range independent environment, with an arbitrary distribution of sources along the z -axis,

$$\left[\frac{\partial^2}{\partial r^2} + \frac{\partial^2}{\partial z^2} + k^2(z) \right] \phi(r, z) = S_\omega \delta(r) \delta(z - z_s), \quad (1)$$

with k being the wavenumber, ϕ the displacement potential, S_ω the source strength and z_s its position. By applying the forward Hankel transform, including the Bessel function J_0 of order 0, with respect to the horizontal wavenumber k_r , defined as,

$$F(k_r, z) = \int_0^\infty f(r, z) J_0(k_r r) r dr, \quad (2)$$

to equation 1, it is transferred to the wavenumber spectrum and reduced by one dimension, yielding the so-called depth-dependent wave equation,

$$\left[\frac{\partial^2}{\partial z^2} + (k^2 - k_r^2) \right] \phi(k_r, z) = \frac{S_\omega}{2\pi} \delta(z - z_s). \quad (3)$$

Given the already mentioned environmental restrictions, analytical solutions for equation 3 can be found, for a number of different source types, including the point sources used later on. In the case of a multi-layered environment, the solutions for equation 3 in each layer can be implemented very efficiently in a numerically stable manner. To finally obtain the desired results in the frequency domain, an inverse Hankel transformation has to be applied. Optionally, as in every frequency domain computation, time domain results can be obtained by an inverse Fourier transformation over a set of frequencies. For a more exhaustive treatment of the used wavenumber integration formulation, the reader is referred to Lippert and Lippert [18].

To illustrate the application of wavenumber integration in the context of pile driving, a Pekeris wave guide with a water depth of 20 m over a fluid half-space representing the bottom is used, adopting the material parameters for the speed of sound c and the density ρ from the example discussed in section 2. To model the inclined wave fronts, which are characteristic of pile driving, the knowledge about their generation can be used to simulate them using a set of point sources, as suggested by Reinhall and Dahl [14]. Doing so, an output signal in the time domain is chosen, which is emitted by the sources. Each source is switched on, the moment the impulse would pass its position. The according time delay can be calculated by the respective distance from the hammer, i.e., the top of the pile, and the velocity of the impulse.

For illustration purposes, the pile length of $L = 30$ m is represented by only six point sources, which is considerably too few to model a closed wave front, but has the advantage, that the single source contributions can be plotted clearly. Each source emits a single sine cycle with a frequency of 100 Hz, with a resulting time offset of $\Delta t = \Delta L/c_{imp} = 1,2$ ms between the sources. In figure 2(a), the contributions of the six sources at $t = 9,6$ ms are depicted separately, whereas in figure 2(b) the resulting wave front is shown. The thin blue lines indicate the interface between the water and the soil, whereas the dashed-dotted black lines indicate the resulting wave fronts which can not fully develop, due to the limited number of sources. Again, it has to be stressed that the high SPLs encountered during pile driving can be explained by the Mach wave effect, as all primary wave fronts of the point sources overlap in this case. If the impulse in the pile was slower than the speed of sound in water, the wave fronts would not overlap and the result would be a severely lower maximum pressure.

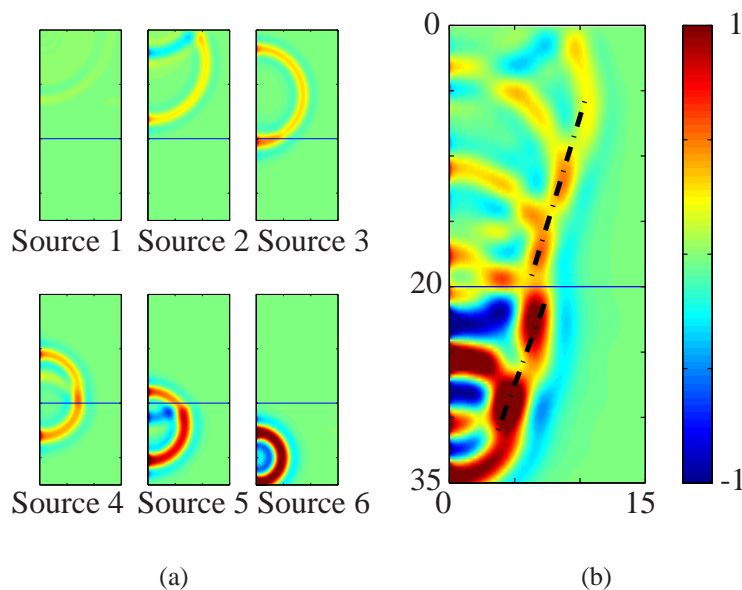


Figure 2. Pressure field contours of single source contributions to a characteristic first pile driving wave front: (a) Single point source contributions for sources placed between $z_{s,1} = 0,1$ m and $z_{s,6} = 29,9$ m / (b) Resulting normalized wave front from all six emitted sine cycles

4. Coupling procedure and comparison of results

The crucial point in coupling the FE results to the WI model is the determination of the excitation of the single point sources. Based on the above considerations, a pressure peak with a period length close to the impact duration of the hammer can be expected, followed by a tailing declining oscillation. The maximum amplitude of this vibration will probably be found shortly after the hammer impact and subsequently decline, as the impulse travels up and down the pile. To get a better insight, the FE model introduced in section 2 is investigated.

Some preliminary considerations have to be made when trying to extract the source signal from the FE simulations. First of all, the nodes to evaluate the signal have to be situated relatively close to the pile to avoid overlapping. Secondly, the desired length of the source signal T_{sig} , after the analytically determined arrival of the impulse in the pile, is decisive for the number of nodes that can be analyzed. Due to the high impulse velocity in the steel pile, it has to be made sure that the impulse has not traveled back to the currently evaluated node and thereby corrupts the signal. Potential boundaries for signal reflections are the end of the pile and the interface between the water and the soil. Therefore, all sources included in the evaluation have to be placed in a safety distance of $L_s = T_{sig} c_{imp}/2$ from both ends of the pile.

Regarding these restrictions, and choosing a signal length of $T_{sig} = 3$ ms, a total number of $N = 62$ nodes can be considered for the described FE model, placed at a distance of 10 cm from the pile. In figure 3(a), the normalized pressure over time of all N nodes after the arrival of the impulse in the pile is shown as a stacked plot. What strikes at first glance is the high resemblance of all signals, hinting to the fact that the impulse, and thereby the acoustic pressure, seems to have a relatively constant shape over time. Further investigation shows, that the maximum signal strength is approximately decreasing exponentially over the traveled distance of the impulse.

As mentioned before, the envisaged model is supposed to be valid up to a frequency of 2 kHz, wherefore the found characteristic signal has to be band-limited. Therefore, each signal is transferred to the frequency domain, processed accordingly by means of a Tukey window, and subsequently transferred back to time domain. A comparison of the original signal p_{FE} and band limited signal p_{lim} is depicted in figure 3(b), for a source depth of $z_s = 17$ m.

For an error analysis, both signals are offset into the positive half-plane by adding the maximum occurring pressure, yielding p_{FE}^* and p_{lim}^* , to avoid the notoriously problematic zero crossings. Defining the error as $e = (p_{FE}^* - p_{lim}^*)/p_{FE}^*$, the mean error over all evaluated source positions is $\bar{e} \approx 2\%$, with the maximum error being $e_{max} \approx 3,6\%$, which is considered an acceptable range.

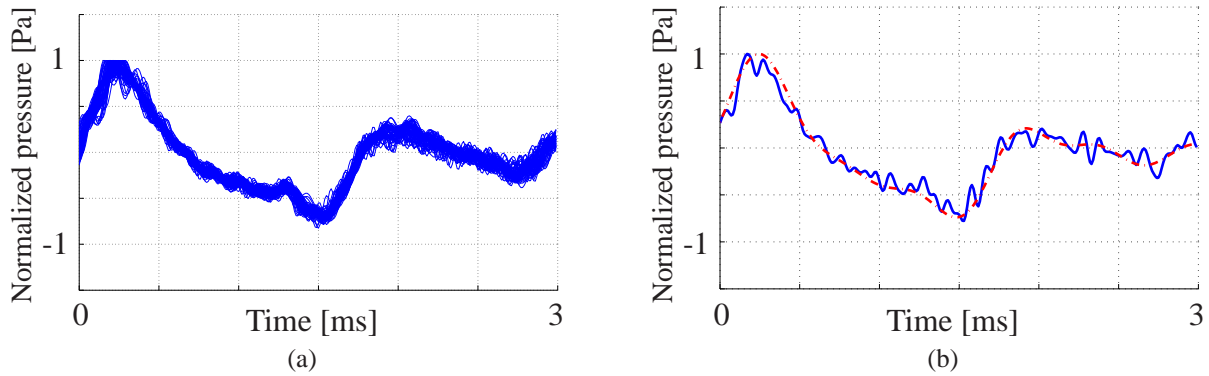


Figure 3. Analysis of the signal emitted by the pile, evaluated at 62 nodes along the pile axis at a distance of 10 cm away from the outer hull of the pile: (a) Stacked plot of normalized FE source signals (b) Exemplary comparison of FE (blue, straight) and band-limited (red, dashed-dotted) signal for a source depth of $z_s = 17$ m

To verify the introduced WI approach, the signals analyzed above are used as input excitation for the WI model and the resulting pressure in some distance from the pile is compared to the according FE results. This is rather challenging since the dimensions of the FE model are limited by practical computational restrictions, while the WI approach is best suited for predictions over long ranges. By evaluating a receiver at $r_{ref} = 40$ m and $z_{ref} = 18$ m, i.e. 2 m above the sea floor, a balance is struck between both restrictions. As input signal for all 27 point sources, equally distributed along the length of the pile, the mean band-averaged signal from all 62 evaluated nodes is taken.

In figure 4(a), the results of the FE and WI simulations are shown for the reference position in the time domain. The time window of the comparison is truncated after 8 ms, as spurious reflections from imperfections at the non-reflecting boundaries in the FE model are corrupting the signal afterwards. Furthermore, both signals are normalized to a maximum amplitude of 1 Pa, as the number of point sources used in the WI model is not yet related to the total energy emitted by the pile. In the scope of these reservations, the signals are found to be in good agreement. The arrivals of the single wave fronts can be identified for both simulations by the positive or negative peaks respectively, which occur approximately at the same time for both models. As expected, the WI results show significantly less high frequency noise, due to the band-limiting of the input signal.

To get a better insight into the degree of accordance of both normalized results, they are transferred to the time domain by means of a narrow-band Fourier transformation and averaged in third-

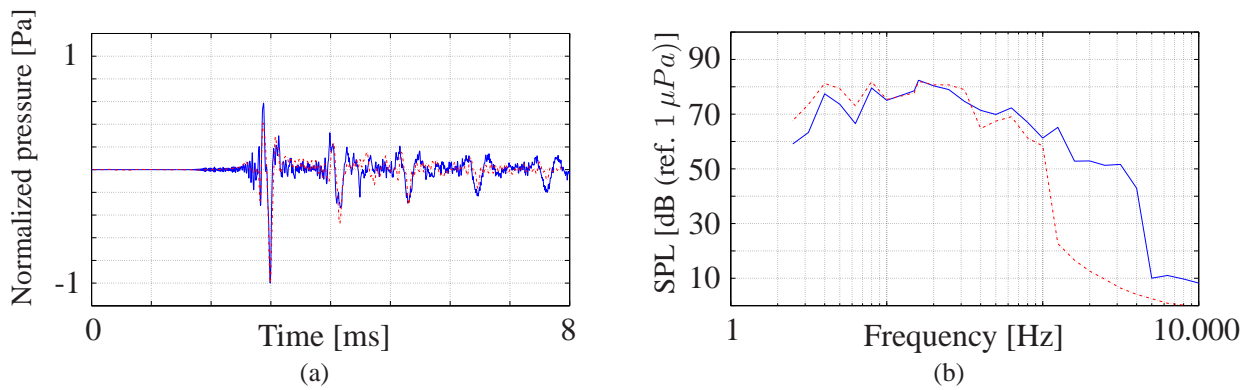


Figure 4. Comparison of finite element (blue) and wavenumber integration (red, dashed-dotted) results at reference position ($r_{ref} = 40 \text{ m} / z_{ref} = 18 \text{ m}$): (a) Normalized pressure vs. time at reference position (b) Comparison of normalized results in the frequency domain, using a third-octave band resolution

octave bands, as depicted in figure 4(b). Again, the signals are found to be in excellent agreement both regarding quality and quantity. The frequency responses at the selected position show the same trend for both models and take on similar values for a wide frequency range. The severe drop in agreement, at frequencies in the range above 1 kHz, is most likely resulting from the band-limiting procedure. Ideally, this would only influence frequencies above 2 kHz, but due to the nature of the Tukey window, the effect already sets in at lower frequencies.

5. Conclusions

An envisaged tripartite model to simulate the acoustic radiation from pile driving has been presented, using a wavenumber integration approach as propagation method. Hereby, one of the key challenges was to determine and verify the acoustic input excitation of this model. Therefore, a transient FE model has been setup and the pressure close to the pile was analyzed and processed for further use in the WI model. Subsequently, the results of both models at a reference position in 40 m distance from the pile have been compared and found to be in excellent agreement, both in time and frequency domain. Hence, it can be assumed that the WI result will also yield reasonable results for receivers in a larger distance from the pile, what is its actual purpose.

As a next step, the acoustic energy radiated from the pile has to be correlated to the emitted energy from the point sources in the WI model, to enable for actual signal comparisons, without prior normalization. Subsequently, parameter studies using, amongst others, different hammer pulses and pile geometries should be performed, to get a deeper insight into the formation of the acoustic signal. Additionally, the validation of the model against results from a recently performed, extensive offshore measurement campaign is planned, to proof its ability of sound pressure level prediction in large distances from the pile.

Acknowledgements

The presented research activities are carried out in the course of the BORA project. The authors gratefully acknowledge the funding of this project by the Federal Ministry for the Environment, Nature Conservation and Nuclear Safety due to an act of the German Parliament (project ref. no. 0325421 A/B/C).

REFERENCES

- ¹ Stadler, J.H. and Woodbury, D.P.. Assessing the effects to fishes from pile driving: Application of new hydroacoustic criteria, *Proceedings of Inter-Noise 2009*, Ottawa, Canada, 26-29 August, (2009).
- ² Götz, T., Hastie, G., Hatch, L.T., Raustein, O., Southall, B.L., Tasker, M. and Thomsen, F., *Overview of the impacts of anthropogenic underwater sound in the marine environment*, OSPAR Commission - Biodiversity Series (2009).
- ³ Bundesministerium für Umwelt, Naturschutz und Reaktorsicherheit. Das Energiekonzept der Bundesregierung 2010 und die Energiewende 2011, (2011).
- ⁴ Koschinski, S and Lüdemann, K. (2011). *Stand der Entwicklung schallminimierender Massnahmen beim Bau von Offshore Windenergieanlagen*. [Online.] available: http://www.bfn.de/habitatmare/de/downloads/berichte/BfN-Studie_Bauschallminderung_Juli-2011.pdf
- ⁵ Umweltbundesamt. Empfehlung von Lärmschutzwerten bei der Errichtung von Offshore-Windenergieanlagen (OWEA), (2011).
- ⁶ Müller, A. and Zerbs, C. (2011). *Offshore wind farms - Measuring instruction for underwater sound monitoring*. [Online.] available: http://www.bsh.de/de/Produkte/Buecher/Standard/Measuring_instruction.pdf
- ⁷ Kastelein, R.A., Bunskoek, P., Hagedoorn, M., Au, W.L. and de Haan, D.. Audiogram of a harbor porpoise (*Phocoena phocoena*) measured with narrow-band frequency-modulated signals, *Journal of the Acoustical Society of America*, **112**, 334–344, (2002).
- ⁸ Kastelein, R.A., Wensveen, P. and Hoek, L.. Underwater hearing sensitivity of harbor seals (*Phoca vitulina*) for narrow noise bands between 0.2 and 80 kHz, *Journal of the Acoustical Society of America*, **126**, 476–483, (2009).
- ⁹ Wilke, F., Klose, K. and Bellmann, M.. *ESRa - Evaluation von Systemen zur Rammschallminderung an einem Offshore-Testpfahl*. Report-Nr. 0325307, (2012).
- ¹⁰ Brekhovskikh, L.M. and Lysanov, Yu.P.. *Fundamentals of Ocean Acoustics*, Springer-Verlag, New York (2003).
- ¹¹ Stokes, A., Cockrell, K., Wilson, J., Davis, D. and Warwick, D.. *Mitigation of Underwater Pile Driving Noise During Offshore Construction: Final Report*. Report-Nr. M09PC00019-8, (2010).
- ¹² Hamilton, E.L.. Geoacoustic modelling of the seafloor, *Journal of the Acoustical Society of America*, **68**, 1313–1340, (1980).
- ¹³ Deeks, A.J. and Randolph, M.F.. A simple model for inelastic footing response to transient loading, *International Journal for Numerical and Analytical Methods in Geomechanics*, **19**, 307–329, (1995).
- ¹⁴ Reinhall, P.G. and Dahl, P.H.. Underwater Mach wave radiation from impact pile driving: Theory and observation, *Journal of the Acoustical Society of America*, **130**, 1209–1216, (2011).
- ¹⁵ Jensen, F.B., Kuperman, W.A., Porter, M.B. and Schmidt, H., *Computational Ocean Acoustics*, Springer-Verlag, New York (2011).
- ¹⁶ Schmidt, H. and Tango G.. Efficient global matrix approach to the computation of synthetic seismograms, *Geophysical Journal of the Royal Astronomical Society*, **84**, 331–359, (1986).
- ¹⁷ Schmidt, H.. *Safari: Seismo-acoustic fast field algorithm for range-independent environments. User's guide*. SACLANTCEN Report no. SR113, (1988).
- ¹⁸ Lippert, T. and Lippert, S.. Modelling of pile driving noise by means of wavenumber integration, *Acoustics Australia*, **40**, 178–182, (2012).